One-proton knockout from ^{16}C at around 240 MeV/nucleon

Y. X. Zhao,[1,2,3] Y. Z. Sun,[1,2] S. T. Wang,[1,2,*] Z. Y. Sun,[1,2] X. H. Zhang,[1,2] D. Yan,[1] D. Y. Pang,[4] P. Ma,[1] Y. H. Yu,[1,2] K. Yue,[1] S. W. Tang,[1,2] S. M. Wang,[1] F. Fang,[1] Y. Sun,[1,2,3] Z. H. Cheng,[1,3] X. M. Liu,[1] H. R. Yang,[1,2] C. G. Lu,[1] and L. M. Duan[1,2]

[1]*CAS Key Laboratory of High Precision Nuclear Spectroscopy, Institute of Modern Physics, Chinese Academy of Sciences, Lanzhou 730000, China*

[2]*School of Nuclear Science and Technology, University of Chinese Academy of Sciences, Beijing 100049, China*

[3]*School of Nuclear Science and Technology, Lanzhou University, Lanzhou 730000, China*

[4]*School of Physics and Nuclear Energy Engineering, Beihang University, Beijing 100191, China*

(Received 16 June 2019; published 17 October 2019)

The cross section for one-proton knockout from ^{16}C with a large neutron-proton separation energy asymmetry on a carbon target has been measured at an intermediate beam energy of around 240 MeV/nucleon. The measured cross section is compared to the predictions based on the eikonal reaction model with shell-model structure inputs. The beam-energy dependence of the reduction on the extracted spectroscopic strength for strongly bound nucleon removal is derived from combining the existing intermediate-energy data with the present measurement. The deduced reduction factor R_s, defined as the ratio of the measured and theoretical cross sections, for the strongly bound nucleon removal at around 240 MeV/nucleon is consistent with the systematics observed from knockout reactions induced by light nuclear targets at intermediate energies of around 80 MeV/nucleon.

DOI: 10.1103/PhysRevC.100.044609

I. INTRODUCTION

For decades, one-nucleon knockout reactions in inverse kinematics at intermediate and high energies have been extensively used to probe the structure of unstable nuclei [1–10]. The reaction studies usually employ light nuclear targets of Be or C and have yielded a significant amount of spectroscopic factor information on nuclei far from stability.

A systematic analysis of a large body of experimental data for knockout reactions based on the eikonal model indicates a strong isospin asymmetry dependence of the reduction of the extracted spectroscopic strength relative to the shell-model predictions [2–4]. The reduction of the spectroscopic strength is characterized by the reduction factor $R_s \equiv \sigma_{\rm exp}/\sigma_{\rm th}$, where $\sigma_{\rm exp}$ is the experimental knockout cross section and $\sigma_{\rm th}$ is the theoretical cross section obtained from the combination of the eikonal theory and the shell model. The isospin asymmetry is quantified by ΔS, the difference between the neutron and proton separation energies of the projectile nuclei ($\Delta S = S_n - S_p$ for neutron removal and $\Delta S = S_p - S_n$ for proton removal). In particular, it is found that the R_s is far less than 1 for removal of strongly bound nucleons. The strong reduction in spectroscopic strength, at first, is suggested to be attributed to the enhanced correlation experienced by strongly bound nucleons that is not taken into account in shell-model calculations [4,11,12].

On the other hand, a weak ΔS dependence of the R_s values is obtained from studies of transfer reactions [13–15] and quasifree scattering reactions [16–18], and the deduced R_s values for strongly bound nucleon removal with these reactions are not strongly reduced, which is contrary to the results from light-nuclear-target-induced knockout reactions. So far, a consensus on the cause of the strong reduction observed in knockout reactions has yet to be established, and it is unsettled whether this strong reduction is an indication of inadequacies in the shell model or deficiencies in the eikonal reaction model.

The high energy of the beam is important for the applicability of the eikonal reaction model that uses the sudden and eikonal approximations and is of particular importance for its applicability to cases involving strongly bound nucleon removal. As is shown in Ref. [9], strong nonsudden effects are observed in the case of strongly bound neutron removal from ^{14}O at a relatively low beam energy of 57 MeV/nucleon. So far, most of the existing data on R_s values for strongly bound nucleon removal induced by light nuclear targets are measured at intermediate energies of around 80 MeV/nucleon. If the underlying theoretical assumptions for the reaction mechanism are reliable at beam energies near to and in excess of 80 MeV/nucleon, the measurements for a given nucleus at different beam energies should yield consistent results on the deduced R_s values. Therefore, it would be of interest and value to study these reactions at higher beam energies, say in excess of 200 MeV/nucleon, to explore the robustness of the deduced R_s values to changes in beam energy.

Experimental studies on light-nuclear-target-induced strongly bound nucleon removal at beam energies of above 200 MeV/nucleon are still scarce. A dedicated experimental work for studying the behavior of R_s at a higher beam

*wangshitao@impcas.ac.cn

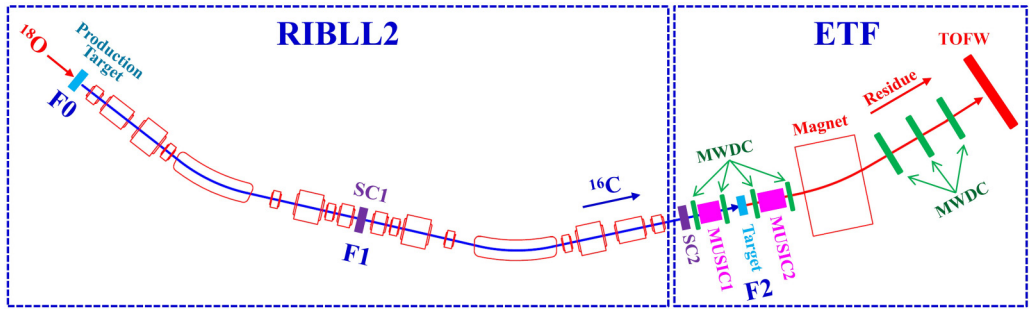

FIG. 1. Schematic view of the layout of the RIBLL2 and the ETF.

energy has been performed recently using the ^{12}C(^{30}Ne, ^{29}F) reaction at 230 MeV/nucleon [19]. However, because of the complexity in the structure of the deformed ^{30}Ne nucleus, the structure inputs introduce much uncertainty for calculations, and thus the obtained conclusion is less clear [19]. In addition, there is a lack of measurement of the (^{30}Ne, ^{29}F) reaction at an intermediate energy of $\approx$ 80 MeV/nucleon for straightforward study of the energy dependence of R_s without additional uncertainties attributed to the structure input.

In this work, we perform a new measurement for strongly bound nucleon removal at an energy above 200 MeV/nucleon, in an effort to further investigate the energy dependence of the R_s for strongly bound nucleon removal. The reaction used is one-proton knockout from ^{16}C on a carbon target at $\approx$ 240 MeV/nucleon. The neutron-rich nucleus ^{16}C is a good testing ground to study the energy dependence of the R_s for strongly bound nucleon removal. First, ^{16}C exhibits large differences in individual nucleon separation energies ($\Delta S = 18.35$ MeV, $S_p = 22.6$ MeV, and $S_n = 4.25$ MeV). Second, the one-proton knockout cross section on ^{16}C is already measured accurately at an intermediate energy of 75 MeV/nucleon [9], allowing a direct comparison, in the same nucleus, of the extracted R_s values at different energies without influence from uncertainties of structure inputs.

II. EXPERIMENT

The experiment was performed at the External Target Facility (ETF) [20] at the Institute of Modern Physics, Chinese Academy of Sciences. A primary beam of ^{18}O was accelerated to 280 MeV/nucleon by the main Cooler Storage Ring (CSRm) synchrotron of the Heavy Ion Research Facility in Lanzhou (HIRFL) [21] and directed onto a Be target of 15-mm thickness. The unstable secondary beams produced by fragmentation of ^{18}O were separated using the Radioactive Ion Beam Line in Lanzhou-II (RIBLL2) [22] and transported to the experimental area where the ETF is located. The layout of the RIBLL2 and the ETF is shown in Fig. 1. The secondary cocktail beams, magnetically centered on ^{16}C, were identified using the TOF-ΔE method. The time of flight $\mathrm{TOF}_{\mathrm{SC1}\rightarrow\mathrm{SC2}}$ was measured between two plastic scintillator detectors (denoted by SC1 and SC2 in Fig. 1) and the energy loss $\Delta E_{\mathrm{MUSIC1}}$ was recorded by a multiple sampling ionization chamber (denoted by MUSIC1 and located at the entrance of the ETF). The particle identification spectrum for the secondary cocktail beams is presented in Fig. 2, from which it can be seen that a clean separation of different constituents of the secondary beams is achieved.

The secondary beams impinged on a 900 mg/cm^2 thick carbon reaction target installed at the target position of the ETF to induce one-proton knockout reactions. The trigger of the data acquisition system was generated only by requiring the coincidence of the signals from SC1 and SC2, both in front of the reaction target. The kinetic energy of ^{16}C at the center of the target was 239 MeV/nucleon. Two multiwire drift chambers (MWDCs), located upstream of the carbon target and each having an active area of 13 $\times$ 13 cm^2, were used to measure the trajectories of the incoming particles.

Downstream from the carbon target, the heavy reaction products as well as the unreacted beam particles were identified using the detector system of the ETF event by event by combining magnetic rigidity ($B\rho$), time of flight (TOF), and energy loss (ΔE). The $B\rho$ of the outgoing charged fragments passing through the ETF magnet was reconstructed from the positions measured using two MWDCs placed upstream and three MWDCs placed downstream of the magnet. The two MWDCs placed upstream of the magnet have the same active area of 13 $\times$ 13 cm^2. Each of the three MWDCs downstream of the magnet has an active area of 80 $\times$ 60 cm^2. The time

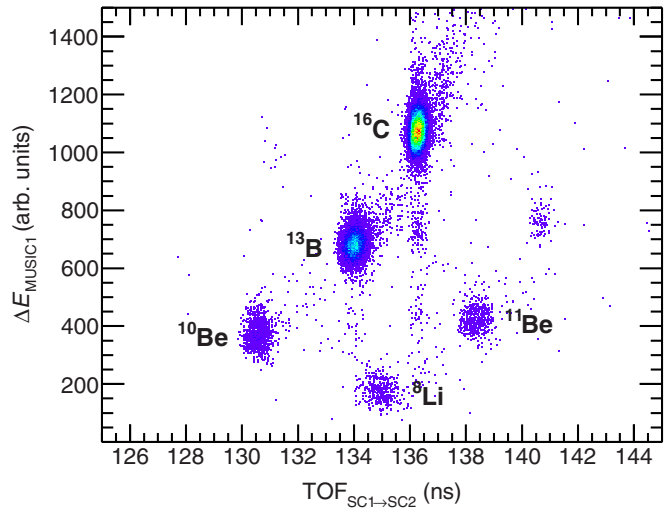

FIG. 2. The particle identification plot for the secondary cocktail beams produced by the RIBLL2.

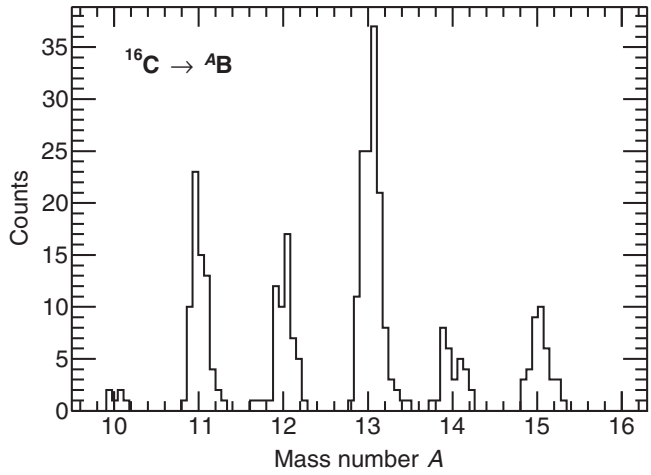

FIG. 3. A typical mass number A identification spectrum for reactions of ^{16}C on a carbon target, measured with the ETF. The particles are already selected for charge number $Z = 5$.

of flight $\mathrm{TOF}_{\mathrm{SC2}\to\mathrm{TOFW}}$ was measured between a plastic scintillator (SC2) and a 30-strip plastic scintillator wall (TOFW) placed about 10 m downstream from the target. The energy loss $\Delta E_{\mathrm{MUSIC2}}$ was measured by a multiple sampling ionization chamber (MUSIC2) placed 50 cm downstream of the reaction target. The nuclear charge number Z of the reaction residues were determined by using the $\Delta E_{\mathrm{MUSIC2}}$ information, while the fragment mass number A values were obtained by applying the relation $B\rho \approx (A/Z)\beta\gamma$, where β and γ denote the velocity v/c and the relativistic Lorentz factor, respectively. A mass resolution of ≈ 0.3 mass units (full width at half maximum), as displayed in Fig. 3, was achieved. With such a resolution the one-proton knockout products ^{15}B can be clearly separated from other boron isotopes. As can be seen in Fig. 3, the counts of the lower mass boron isotopes $^{11-13}$B are higher than those for neutron-rich ^{14,15}B. This is because the cross sections for producing lower mass $^{11-13}$B isotopes may receive large contributions arising from neutron evaporation from unbound excited states of neutron-rich ^{14,15}B isotopes, which have low neutron separation energies.

The acceptance of the ETF detector system for the ^{15}B fragments amounted to $\approx 100\%$. The detection efficiency of the ETF was calibrated using the various secondary beams, and the derived efficiencies were 80%–90%, depending on the charge number of the beam particles. The inclusive cross section for one-proton knockout from ^{16}C to ^{15}B was derived from the yield of detected ^{15}B residues and the number of incoming ^{16}C projectiles, taking into account the density of the carbon target. The obtained inclusive cross section was $\sigma_{\mathrm{exp}}(^{16}\mathrm{C} \to {}^{15}\mathrm{B}) = 16(2)$ mb. To avoid effects arising from reactions on the target frame, the beam-spot size on the target was limited to 4 cm in diameter in the off-line analysis by setting a software gate using the information from the MWDCs. The background contributions were measured by using target-out runs and subtracted. The quoted uncertainties are dominated by statistical errors, while systematic errors mainly arise from the correction for the ETF detection efficiency and are added to the statistical uncertainty in quadrature.

III. THEORETICAL ANALYSIS AND DISCUSSION

The theoretical cross sections for the one-proton removal reaction on ^{16}C are calculated using the eikonal reaction theory with shell-model structure inputs. The theoretical cross sections to each final state, with spin-parity J^π, of the residue (core) nucleus are calculated using [1]

$$\sigma_{\mathrm{th}} = \sum_{nlj} \left[\frac{A}{A-1}\right]^N C^2S(J^\pi, nlj)\sigma_{\mathrm{sp}}\left(nlj, S_p^{\mathrm{eff}}\right), \qquad (1)$$

where C^2S is the shell-model spectroscopic factor for the removed proton with respect to the core state, σ_{sp} denotes the single-particle cross section calculated using the eikonal model assuming the unit spectroscopic factor [1], nlj are the quantum numbers of the removed proton, S_p^{eff} is the effective proton separation energy to the given final state, and $[A/(A-1)]^N$ is the center-of-mass correction factor with A being the mass number of the projectile and N the oscillator quantum number associated with the major shell of the removed proton.

The σ_{sp} includes contributions from both elastic and inelastic breakup mechanisms and is computed using the computer code MOMDIS [23]. The valence-proton wave function is calculated using a Woods-Saxon potential well of a fixed geometry. A diffuseness of $a_0 = 0.7$ fm is adopted, as used in Ref. [24]. Because the calculated cross section is sensitive to the choice of the radius parameter r_0, different r_0 values ranging from 1.15 to 1.35 fm are used in the calculations for comparison. As is shown below, the choice of r_0 does not affect the relative cross sections from different beam energies. The depth of the potential is determined to reproduce the experimental proton separation energy S_p. The proton- and residue-target elastic S matrices are calculated with the "t-ρ-ρ" approximation [25] using the parametrized nucleon-nucleon scattering amplitudes and nucleon density distributions of the core and target nuclei. The nucleon density distribution of the ^{15}B core is obtained from a Hartree-Fock calculation employing the SkX interaction [26]. The densities of the ^{12}C (^{9}Be) target nuclei are chosen to be of Gaussian form with a rms matter radius of 2.32 (2.36) fm [24].

In ^{15}B, three bound states are predicted by the shell model and are confirmed experimentally [27]. The ground state has a spin-parity of $3/2^-$ with a $\pi 0p_{3/2}$ hole configuration, and the two excited states, $(5/2^-)$ and $(7/2^-)$, are interpreted as configurations originating from the coupling of a $\pi 0p_{3/2}$ hole to the 2^+ excited state in ^{16}C. Therefore, among these three bound states of ^{15}B, only the ground state is expected to be populated in direct one-proton removal from ^{16}C. The spectroscopic factor C^2S of 2.95 for $\pi 0p_{3/2}$ knockout from ^{16}C to the ground state of ^{15}B is taken from Ref. [9], where shell-model calculations with the WBT interaction in the *psd* valence space were performed [28].

The calculated cross sections σ_{th} using different radius parameter r_0 values for one-proton knockout from the $\pi 0p_{3/2}$ orbit of ^{16}C to the $3/2^-$ ground state of ^{15}B at 75 and 239 MeV/nucleon are presented in Table I. It can be seen that a change of 0.1 fm in r_0 leads to $\approx 10\%$ variation in the calculated cross sections and thus results in a $\approx 10\%$ effect in the absolute R_s deduced. Nevertheless, it is found that

TABLE I. The measured and calculated cross sections for one-proton knockout from the $\pi 0p_{3/2}$ orbit of ^{16}C to the $3/2^-$ ground state of ^{15}B and the resulting reduction factors R_s. In the calculations, three different radius parameter r_0 values are used.

Beam energy		σ_{th} (mb)			R_s		
(MeV/nucleon)	σ_{exp} (mb)	$r_0 = 1.15$ fm	$r_0 = 1.25$ fm	$r_0 = 1.35$ fm	$r_0 = 1.15$ fm	$r_0 = 1.25$ fm	$r_0 = 1.35$ fm
75	18(2)[a]	55.8	61.4	67.5	0.32(3)	0.29(3)	0.27(3)
239	16(2)[b]	49.4	53.9	58.9	0.32(3)	0.30(3)	0.27(3)
	14.4(20)[c]				0.29(3)	0.27(3)	0.24(3)

[a]Reference [9].
[b]Assume that the cross section to the ground state of ^{15}B is equal to 100% of the inclusive cross section.
[c]Assume that the cross section to the ground state of ^{15}B is equal to 90% of the inclusive cross section.

the relative values for the calculated cross sections from the two energies remain almost unchanged when using different r_0 values. Hence, the choice of r_0 has a weak effect on the deduced beam energy dependence of the R_s values.

In the ^{9}Be(^{16}C, ^{15}B) reaction at 75 MeV/nucleon, the measured cross section to the ground state of ^{15}B is $\sigma_{exp}(75) = 18(2)$ mb [9]. It is worthwhile to note that the two excited states of ^{15}B, which are not expected to be populated by proton removal, are also populated experimentally with a small cross section of 2 mb [9]. For the ^{12}C(^{16}C, ^{15}B) reaction at 239 MeV/nucleon, only the inclusive cross section is measured. We therefore make an assumption that 90% of the inclusive cross section feeds the ground state of ^{15}B according to the measured cross-section branching ratio at 75 MeV/nucleon, and then the partial cross section to the ground state of ^{15}B at 239 MeV/nucleon is deduced to be $\sigma_{exp}(239) = 14.4(20)$ mb. We also make another hypothesis that the ground state takes 100% of the inclusive cross section, resulting in $\sigma_{exp}(239) = 16(2)$ mb.

The deduced R_s values for the (^{16}C, ^{15}B) reactions at 75 and 239 MeV/nucleon based on different assumptions are listed in Table I. A scatter of the R_s data points in the range of 0.24–0.32 can be seen. Despite a large degree of scatter on these values, the results are consistent with the systematics for the R_s values with $\Delta S \approx 18$ MeV, as shown in Fig. 1 of Ref. [2]. Furthermore, the deduced ratio of the R_s values at the two beam energies [$R_s(239)/R_s(75)$] are nearly independent of the parameter r_0 chosen, as shown in Fig. 4. Assuming $\sigma_{exp}(239) = 16(2)$ mb, the deduced ratio $R_s(239)/R_s(75)$ is near unity. The deduced ratio $R_s(239)/R_s(75)$ is slightly smaller than unity when assuming $\sigma_{exp}(239) = 14.4(20)$ mb.

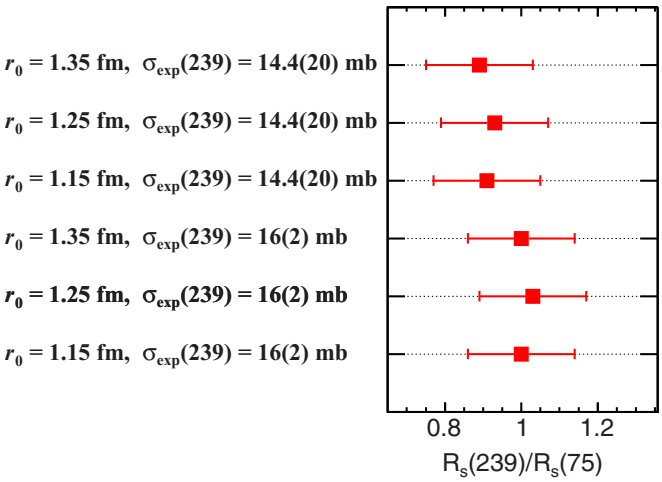

FIG. 4. The ratio of the R_s extracted at 239 MeV/nucleon to that at 75 MeV/nucleon with different theoretical and experimental inputs.

The present results suggest that the R_s values do not have evident dependence on beam energy and imply that the R_s values are robust to changes in beam energy at the intermediate-energy region. This adds further confidence to the application of the eikonal model in knockout reactions at beam energies of near or above 80 MeV/nucleon. However, we note that the validity of the eikonal reaction model description needs further tests at even higher energies. It also should be noted that the quasifree scattering of oxygen isotopes in Ref. [16] was performed at a higher energy of around 400 MeV/nucleon. Even though the reason for the strong reduction of R_s remains unsolved, it has been shown that the one-nucleon knockout methodology based on the eikonal model and shell model can be reliably used to predict the one-nucleon knockout cross sections by applying a scale factor of R_s extracted from the systematics of the relation between R_s and ΔS [29,30].

IV. SUMMARY

In summary, the cross section was measured for light-nuclear-target-induced one-proton knockout in the neutron-rich nucleus ^{16}C at an intermediate energy of 240 MeV/nucleon. The present measurement together with the intermediate-energy one-proton knockout data on ^{16}C provides a good opportunity to study the energy dependence of the reduction factor R_s. A small measured knockout cross section for the strongly bound valence proton as compared to theoretical calculations implies a very small R_s, in line with the results that have been observed in similar knockout analyses with intermediate energies of ≈ 80 MeV/nucleon. The results indicate the robustness of the deduced R_s values to changes in beam energy, lending credence to the eikonal model theory. However, the discrepancies between the knockout reaction and other reactions still remain unsolved. There is, of course, still the possibility that the simplified eikonal reaction model description overestimates the

one-nucleon removal cross sections for strongly bound nucleons at beam energies of the present measurement. Therefore, further assessments of the reaction model are desirable. For example, in the case of deeply bound proton knockout in the presence of weakly bound neutrons, it is questionable whether the surface neutrons would remain unperturbed, i.e., behave as a "spectator."

ACKNOWLEDGMENTS

The authors thank the HIRFL accelerator staff for preparing the primary and secondary beams. This work was supported by the National Natural Science Foundation of China (Grants No. 11575257, No. U1732134, and No. 11305222) and the open research project of CAS large research infrastructures.

[1] P. G. Hansen and J. A. Tostevin, Annu. Rev. Nucl. Part. Sci. **53**, 219 (2003).
[2] J. A. Tostevin and A. Gade, Phys. Rev. C **90**, 057602 (2014).
[3] A. Gade *et al.*, Phys. Rev. C **77**, 044306 (2008).
[4] A. Gade *et al.*, Phys. Rev. Lett. **93**, 042501 (2004).
[5] B. A. Brown, P. G. Hansen, B. M. Sherrill, and J. A. Tostevin, Phys. Rev. C **65**, 061601(R) (2002).
[6] D. Bazin *et al.*, Phys. Rev. Lett. **102**, 232501 (2009).
[7] K. Wimmer, D. Bazin, A. Gade *et al.*, Phys. Rev. C **90**, 064615 (2014).
[8] G. F. Grinyer *et al.*, Phys. Rev. Lett. **106**, 162502 (2011).
[9] F. Flavigny, A. Obertelli, A. Bonaccorso, G. F. Grinyer, C. Louchart, L. Nalpas, and A. Signoracci, Phys. Rev. Lett. **108**, 252501 (2012).
[10] C. Wen *et al.*, Chin. Phys. C **41**, 054104 (2017).
[11] Ø. Jensen, G. Hagen, M. Hjorth-Jensen, B. A. Brown, and A. Gade, Phys. Rev. Lett. **107**, 032501 (2011).
[12] R. J. Charity, L. G. Sobotka, and W. H. Dickhoff, Phys. Rev. Lett. **97**, 162503 (2006).
[13] J. Lee *et al.*, Phys. Rev. Lett. **104**, 112701 (2010).
[14] F. Flavigny *et al.*, Phys. Rev. Lett. **110**, 122503 (2013).
[15] Y. P. Xu *et al.*, Phys. Lett. B **790**, 308 (2019).
[16] L. Atar *et al.*, Phys. Rev. Lett. **120**, 052501 (2018).
[17] M. Gómez-Ramos and A. M. Moro, Phys. Lett. B **785**, 511 (2018).
[18] S. Kawase *et al.*, Prog. Theor. Exp. Phys. **2018**, 021D01 (2018).
[19] J. Lee *et al.*, Prog. Theor. Exp. Phys. **2016**, 083D01 (2016).
[20] Y. Z. Sun *et al.*, Nucl. Instrum. Methods Phys. Res., Sect. A **927**, 390 (2019).
[21] J. W. Xia *et al.*, Nucl. Instrum. Methods Phys. Res., Sect. A **488**, 11 (2002).
[22] B.-H. Sun *et al.*, Sci. Bull. **63**, 78 (2018).
[23] C. A. Bertulani and A. Gade, Comput. Phys. Commun. **175**, 372 (2006).
[24] E. C. Simpson and J. A. Tostevin, Phys. Rev. C **79**, 024616 (2009).
[25] J. S. Al-Khalili, J. A. Tostevin, and I. J. Thompson, Phys. Rev. C **54**, 1843 (1996).
[26] B. A. Brown, Phys. Rev. C **58**, 220 (1998).
[27] M. Stanoiu *et al.*, Eur. Phys. J. A **22**, 5 (2004).
[28] E. K. Warburton and B. A. Brown, Phys. Rev. C **46**, 923 (1992).
[29] A. Gade, R. V. F. Janssens, J. A. Tostevin, D. Bazin, J. Belarge, P. C. Bender, S. Bottoni, M. P. Carpenter, B. Elman, S. J. Freeman, T. Lauritsen, S. M. Lenzi, B. Longfellow, E. Lunderberg, A. Poves, L. A. Riley, D. K. Sharp, D. Weisshaar, and S. Zhu, Phys. Rev. C **99**, 011301(R) (2019).
[30] A. Gade *et al.*, Phys. Rev. Lett. **122**, 222501 (2019).